# Operando kinetics of hydrogen evolution and elemental dissolution : A time resolved mass-charge balance during the anodic dissolution of magnesium with variable iron content

Baojie Dou, Xuejie Li, Junsoo Han, Nick Birbilis, Kevin Ogle

# *Operando* kinetics of hydrogen evolution and elemental dissolution Ⅱ:A time resolved mass-charge balance during the anodic dissolution of magnesium with variable iron content


Baojie Dou, Xuejie Li, Junsoo Han, Nick Birbilis, Kevin Ogle

PII: S0010-938X(23)00137-3

DOI: https://doi.org/10.1016/j.corsci.2023.111095

Reference: CS111095

To appear in: *Corrosion Science*

Received date: 6 December 2022
Revised date: 15 February 2023
Accepted date: 6 March 2023

Please cite this article as: Baojie Dou, Xuejie Li, Junsoo Han, Nick Birbilis and Kevin Ogle, *Operando* kinetics of hydrogen evolution and elemental dissolution Ⅱ:A time resolved mass-charge balance during the anodic dissolution of magnesium with variable iron content, *Corrosion Science,* (2022) doi:https://doi.org/10.1016/j.corsci.2023.111095

# *Operando* kinetics of hydrogen evolution and elemental dissolution II: A time resolved mass-charge balance during the anodic dissolution of magnesium with variable iron content

Baojie Dou [a, b], Xuejie Li [a,c], Junsoo Han [d], Nick Birbilis [e], Kevin Ogle [a]*

a) Chimie ParisTech, PSL University, CNRS, Institut de Recherche Chimie Paris (IRCP), F-75005, Paris, France
b) School of Materials Science and Engineering, Sichuan University of Science & Engineering, 643000, Zigong, China
c) Department of Chemistry, Western University, London, ON, N6A 5B7, Canada
d) Sorbonne Université, Laboratoire Interfaces et Systèmes Electrochimiques, LISE, F-75005, Paris, France
e) Faculty of Science, Engineering and Built Environment, Deakin University, Waurn Ponds, VIC.3216, Australia

**Corresponding author. E-mail: kevin.ogle@chimieparistech.psl.eu (Kevin Ogle)*

**Abstract**

The rates of hydrogen evolution, magnesium (Mg) dissolution and electron exchange were monitored individually, *in situ*, and in real time during anodic and cathodic polarization of Mg in 0.1 M NaCl. Under all conditions, the anodic charge correlated with $Mg^{2+}$ dissolution while hydrogen formation was independent and led to insoluble Mg(II). Increased iron (Fe) impurity promoted hydrogen evolution, but was not necessary for the negative difference effect. These results suggest that electrochemical dissolution occured across an intact Mg(II)-based film, while hydrogen evolution occurred in regions where the film breaks down induced by anodic polarization.

## 1. Introduction

The anodic polarization of Mg results in an enhanced hydrogen evolution reaction (HER) rate which increases with increasing anodic current, commonly referred to as the negative difference effect (NDE). Despite having been discovered more than 150 years ago [1], the origins of the NDE remain under debate. Possible mechanisms have emerged and have been recently reviewed [2,3,4]. Although the effect has been observed on other materials such as Al [5] and rare earth elements [6], hydrogen evolution during anodic polarization is especially intense for Mg. Understanding this effect is important on the basis that Mg is the lightest structural metal, and corrosion limits its use for many applications in which it would otherwise be an ideal candidate. More specifically, the evolution of hydrogen during Mg dissolution also limits the use of Mg as an anode material in batteries or sacrificial anodes [7,8,9,10]. In such applications, hydrogen evolution is a parasitic reaction on the anode, resulting in a loss of efficiency.

A key to understanding the mechanism of so-called NDE, which refers to hydrogen evolved during anodic polarization, is obtaining the correct stoichiometry between charge passed, hydrogen evolved, and oxidized Mg. The term "NDE" refers to the mass-charge balance [11], the observation that the total quantity of oxidized Mg formed as a result of anodic polarization, is greater than that predicted by the anodic charge consumed during polarization. The excess Mg oxidation is, of course, compensated by hydrogen evolution (NDE). The stoichiometry of the reaction requires considering the oxidation of Mg to form either dissolved Mg ions ($Mg^{2+}$(aq), **Eq. 1**), or insoluble Mg oxide/hydroxide (Mg(II), in this case $Mg(OH)_2$(s), **Eq. 2**). The oxidation is balanced by hydrogen ($H_2$(g)) evolution (**Eq. 3**) and electron transfer (**Eqs. 1-3**). A simple overall reaction scheme highlighting these processes is as follows:

$$Mg \rightarrow Mg^{2+}(aq) + 2\ e^- \quad [1]$$

$$Mg + 2\ OH^- \rightarrow Mg(OH)_2(s) + 2\ e^- \quad [2]$$

$$2\ H_2O + 2\ e^- \rightarrow 2\ OH^- + H_2(g) \quad [3]$$

If the rates of the above reactions are expressed electrical currents according to Faraday's law, the total electrical current measured during anodic polarization in the absence of any competing redox reactions, is written as:

$$i_e = i_{Mg^{2+}} + i_{Mg(II)\text{-}ox} - i_{H_2} \quad [4]$$

where $i_e$ is the faradaic electrochemical current, $i_{Mg^{2+}}$ and $i_{H_2}$, are the dissolution rate of Mg and the hydrogen evolution rate, expressed as electrochemical currents. The difference, expressed as a current $i_{Mg(II)\text{-}ox}$, is the formation of insoluble Mg oxidation products. Much of the literature regarding NDE has focused on average mass balance measurements that may be obtained by total charge, total hydrogen produced, and mass loss following removal of corrosion products obtained after relatively long periods of time. This was the case for the original experiments of Beetz [1]. Time resolved measurements are more insightful for identifying possible mechanisms, as they permit direct correlation between the different terms during transient experiments. A complete time dependent evolution of a Mg alloy during anodic polarization requires measuring at least three of the aforementioned coupled phenomena, along with the total electron transfer rate. Time resolved measurements have been recently presented involving two of the terms in **Eq. 4**, electron transfer ($i_e$) and coupled with either Mg dissolution rate ($i_{Mg^{2+}}$) using atomic spectroelectrochemistry [12,13,14,15,16], or hydrogen evolution ($i_{H_2}$) using the gravimetric technique originally developed by Curioni [17,18,19,20]. These methods have provided considerable insight into the nature of the reactions, but leave one of the elementary processes undetermined.

The time resolved measurement of the three physical quantities; electric current, elemental dissolution, and hydrogen evolution; was first attempted by Lebouil *et al.* [13,14]. A micro-fluidic system was equipped with a video recorder and a specialized image analysis software to quantitatively measure hydrogen bubbles in transit to a downstream inductively coupled atomic emission spectrometer (ICP-AES) for measuring $Mg^{2+}$ concentration. Such work revealed that Mg dissolution rate ($i_{Mg^{2+}}$) and

the anodic faradaic current ($i_e$) were in good correlation, with a stoichiometry consistent with a direct, n = 2, dissolution step (**Eq. 1**). By contrast, the rate of anodic hydrogen production (the rate of the NDE, $i_{H_2}$) increased throughout the experiment and did not seem to be directly associated with the Mg dissolution rate. These results strongly suggested that the electrochemical Mg dissolution (**Eq. 1**) and the NDE were not directly related.

It was proposed that the electrochemical Mg dissolution (**Eq. 1**) occurred across an intact oxide/hydroxide film leading to a time independent stoichiometry of n = 2 between $e^-$ and $Mg^{2+}(aq)$ [13, 14]. Concomitantly, the passage of anodic current would lead to the formation of defects within the film where Mg(0) would contact $H_2O$, leading to an essentially instantaneous reaction to form insoluble corrosion products due to the high thermodynamic affinity of Mg to react with water (E° = -2.38 V vs. SHE):

$$Mg + 2\ H_2O \rightarrow Mg(OH)_2(s) + H_2(g) \quad [5]$$

$$Mg + H_2O \rightarrow MgO(s) + H_2(g) \quad [6]$$

This close relationship between $i_e$ and $i_{Mg^{2+}}$ had also been observed in previous studies with in-line dissolution experiments, albeit in which hydrogen was not measured [12-14]. Further, in the original 19th century work of Beetz [1], it was noted that the solid oxidized Mg products formed were stoichiometrically in agreement with the hydrogen produced. However, the complete time resolved mass-charge balance experiments of Lebouil *et al.* [13,14] were conducted over a limited range of conditions and with only one Mg specimen containing a non-negligible impurity level of Fe (280 ppm). The generality of the mechanisms proposed therein was not fully demonstrated.

In part I of this work [21] a novel adaptation of the AESEC – gravimetric hydrogen experiment [22], was demonstrated. The quantitative relationship between hydrogen production either by application of cathodic polarization or due to spontaneous open circuit dissolution of a galvanized steel was demonstrated. The objective of the present study is to determine the complete stoichiometry (electron transfer, Mg dissolution, and hydrogen evolution) for Mg in 0.1 M NaCl over a wide range of potential and current to

both refine and supplement the conclusions of Lebouil *et al.* [13,14]. Further, Mg specimens with a varying concentration of Fe were considered, ranging from ultra-high purity (25 ppmw Fe), typical (220 ppmw Fe), and high impurity (13000 ppmw Fe; 1.3 wt.% Fe) so as to separate the intrinsic NDE from that due to the enrichment of noble impurities such as Fe.

## 2. Experimental

### *2.1. Materials*

Magnesium specimens with different concentrations of Fe (25 ppmw Fe, 220 ppmw Fe and 13000 ppmw Fe) were fabricated using a resistance furnace and a crucible capable of producing 300 g ingots. The impurity of 25 ppmw Fe was chosen as this would be approximately the technological limit level of purity of Mg alloys. The 220 ppmw may be equivalent to an approximate technical grade that would be used in most Mg alloy applications. The 13000 ppmw Fe sample represents a high impurity Mg sample. A complete description is available in a previous publication [16] and the composition of each alloy used in this work is summarized in **Table 1**. A nominally pure Mg (25 ppmw Fe) was used as the raw material, and a small amount of Fe was added with regular stirring to achieve a specific Fe level in the final casting. AM-Cover™ was employed as a cover gas to reduce oxidation during the melting and casting process. The melt was poured into a graphite-coated cast Fe mold and allowed to air cool. Prior to experiments, the alloys were ground with P2400 grit SiC paper under ethanol and then dried under flowing high purity $N_2$ gas. All solutions were prepared from analytical grade reagents and with high purity deionized water of 18.2 MΩ cm resistivity supplied from Millipore™ system.

**Table 1**. Composition of Mg alloy used in this study. Compositions are given in wt.%, adapted from [16].

| Sample | Mg | Fe | Mn | Zr | Ni | Cu | Al |
|---|---|---|---|---|---|---|---|

| | | | | | | | |
|---|---|---|---|---|---|---|---|
| Mg-25 ppmw Fe | Bal. | 0.0025 | 0.017 | 0.007 | <0.002 | <0.005 | 0.085 |
| Mg-220 ppmw Fe | Bal. | 0.022 | 0.008 | 0.001 | <0.002 | <0.005 | 0.002 |
| Mg-13000 ppmw Fe | Bal. | 1.30 | 0.022 | 0.001 | <0.002 | <0.005 | 0.005 |

*2.2. AESEC measurements*

The principles of the AESEC technique and flow cell have been described in detail previously [[23]]. The dissolution rate of each element in the specimens studied was measured independently and simultaneously, as a function of time, using an inductively coupled plasma atomic emission spectrometer (ICP-AES) downstream from an electrochemical flow cell. This technique permits the direct measurement of elements entering the electrolyte either spontaneously or with electrochemical polarization. In this work, an Ultima 2C$^{TM}$ spectrometer (Horiba Jobin Yvon, France) was used for the online elemental analysis. The emission of Mg and Fe were measured at 279.08 nm and 259.94 nm respectively.

The coupling of the gravimetric hydrogen system with AESEC was described in Part I of this study [[21]]. Mass changes were recorded using a Mettler Toledo ME204$^{TM}$ balance with ± 0.1 mg sensitivity and time resolution of 1 point per second. A Gamry Reference 600$^{TM}$ potentiostat / galvanostat was used to perform the electrochemical experiments. A saturated calomel electrode (SCE) reference electrode and a Pt foil counter electrode with a dimension of 25 × 20 × 0.2 mm were used in all experiments. The electrolyte was 0.1 M NaCl (unbuffered) and samples were exposed to the flowing electrolyte with a 1 cm$^2$ surface. The rate of $H_2$ evolution was calculated using a moving average of 150 s, and data treatment was according to methods described in Part I of this study.[[21]]

## 3. Results and Discussion

*3.1. Potential dependence of Mg dissolution*

An overview of the Mg dissolution and hydrogen evolution rates as a function of potential of the three Mg materials was obtained by consideration of the potentiodynamic elemental polarization curves, shown in **Fig. 1**, for 0.1 M NaCl. The spontaneous Mg dissolution rate in open circuit conditions is shown before and after the potentiodynamic polarization (which is defined as linear sweep voltammetry, LSV). The electrical current density ($i_e$) is displayed, along with the Mg dissolution rate ($i_{Mg^{2+}}$) and the hydrogen evolution rate ($i_{H_2}$), determined from the spectroscopic and gravimetric data, respectively. The elemental dissolution rate is presented as an equivalent current assuming n = 2, whereby $i_M = nF\,\upsilon_M$, and $\upsilon_M$ is the rate of production for M, and F is Faraday constant (96500 C $mol^{-1}$). Note that for simplicity $i_{H_2}$ is defined as a positive value.

The overall effect of the applied potential on the HER and Mg dissolution, as well as their stoichiometry relative to electron exchange, may be readily observed from the experiments herein (**Fig. 1**). In the region of cathodic polarization, the HER rate decreased with increasing potential and closely followed the cathodic current revealing the anticipated $e^-/H_2$ stoichiometry of 2 (**Eq. 3**). In this region of cathodic polarization, $i_{H_2}$ at a given potential was approximately a factor of two less intense for the Mg - 25 ppmw Fe alloy (**Fig. 1a**), but was similar for the other two Fe concentrations (**Figs. 1b** and **1c**), indicative of the enhanced cathodic reaction rate due to the presence of Fe.

In the region of anodic polarization, the Mg dissolution rate ($i_{Mg}$) closely followed the anodic current demonstrating an $e^-/Mg^{2+}(aq)$ stoichiometry of 2 as was observed in prior studies [12-16]. The NDE was clearly visible as the $i_{H_2}$ increased with increasing potential in this region of anodic polarization. The NDE was most pronounced for higher Fe containing specimens (**Figs. 1b** and **1c)** for which the HER ($i_{H_2}$) was more

intense than the anodic current ($i_e$) and the Mg dissolution rate ($i_{Mg} = i_{Mg^{2+}}$). Note that $i_{Mg^{2+}}$ in this work is presented as $i_{Mg}$.

(a)

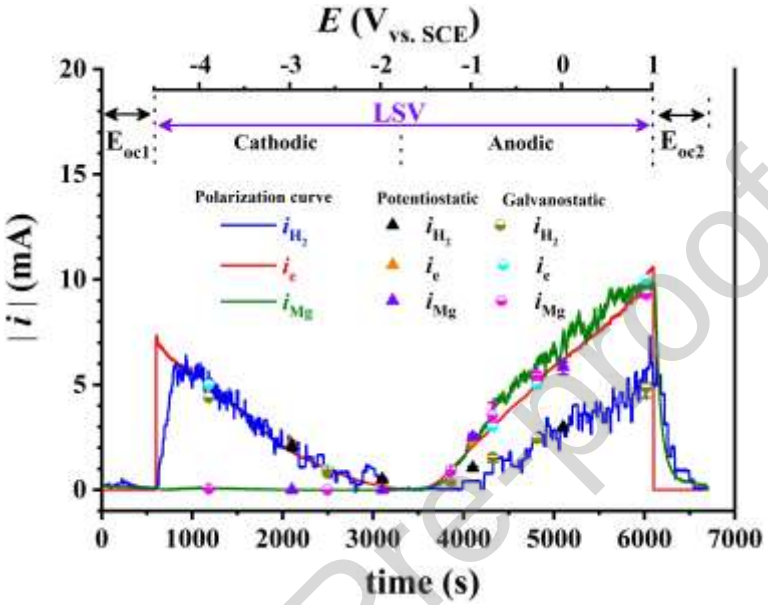


(b)

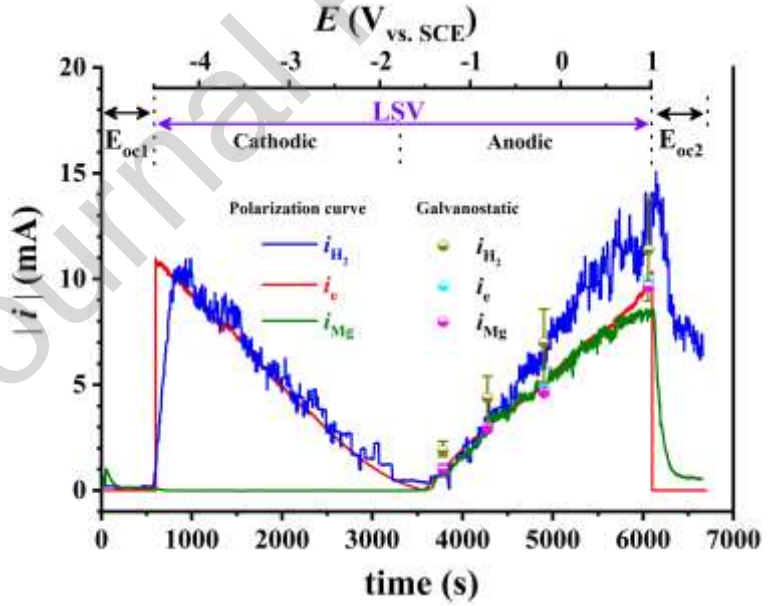


(c)

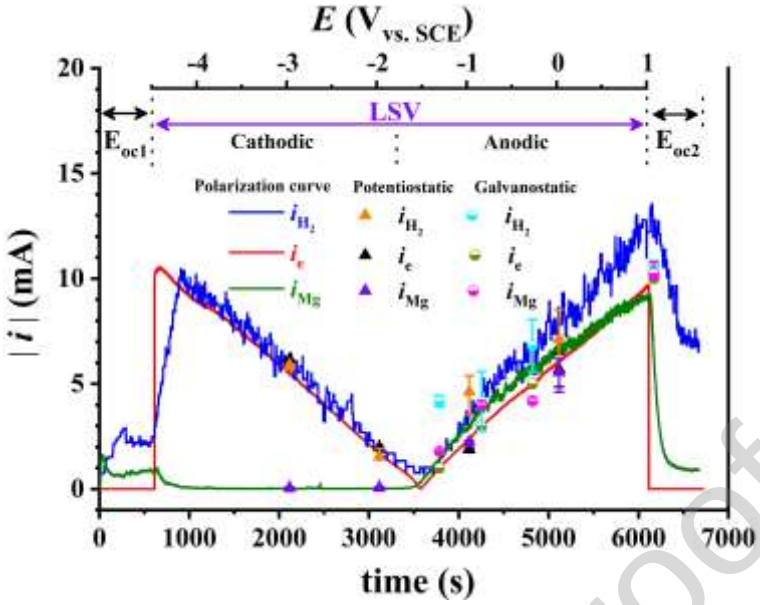


**Fig. 1.** Potentiodynamic linear sweep voltammetry (LSV) curves of Mg alloys in 0.1 M NaCl solution at 1 mV $s^{-1}$ scan rate from -4.5 V to 1.0 V vs. SCE. (a) Mg - 25 ppmw Fe, (b) Mg - 220 ppmw Fe, and (c) Mg - 13000 ppmw Fe. Data in dots are from galvanostatic / potentiostatic measurements shown in **Figs. 2, 4** and **6**. The error bars are obtained from the standard deviation of the signal.

To further supplement the findings from the potentiodynamic experiments reported in **Fig. 1**, galvanostatic and potentiostatic experiments were also performed at various applied potentials and currents. These experiments were performed with the same protocol, replacing the LSV phase of **Fig. 1** with a potentiostatic or galvanostatic hold for 1200 s. Note that the approximate steady state values of $i_{Mg}$ and $i_{H_2}$ obtained from the potentiostatic and galvanostatic experiments are also plotted as discrete points in **Fig. 1** to illustrate the agreement between the two experiments. It is clear that the potentiostatic and potentiodynamic experiments yield a similar potential dependence of Mg dissolution and HER rates.

### *3.2. HER and Mg dissolution during cathodic polarization*

**Fig. 2** shows the rate vs. time profiles obtained for a series of cathodic galvanostatic experiments. The HER rate ($i_{H_2}$) varied within experimental error as predicted from the applied cathodic current by Faraday's law for the reduction of water (**Eq. 3**) and was stable throughout. This confirms the reliability of the measurements for $i_{H_2}$ of Mg using

the AESEC-gravimetric technique both in terms of the quantitative nature of the measurement as well as its stability. This is important as no such reference prediction is possible for $i_{H_2}$ during an anodic polarization.

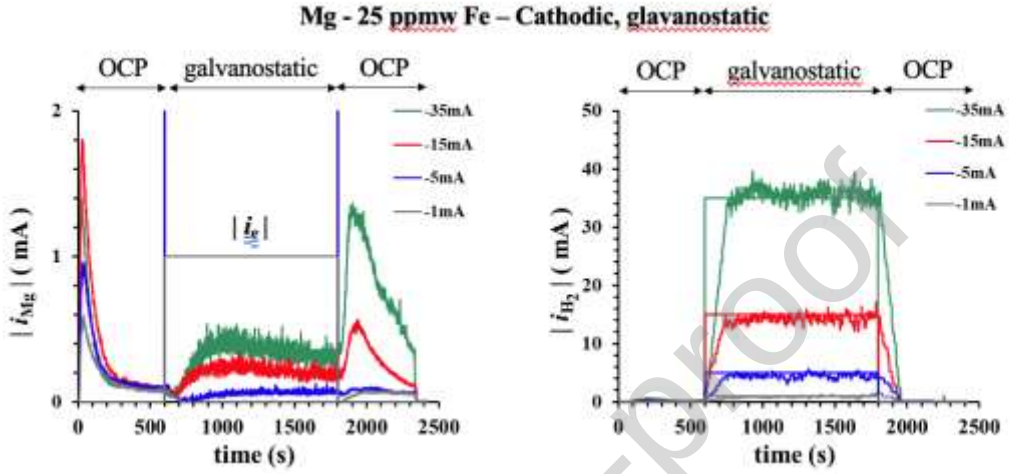


**Fig. 2.** Galvanostatic cathodic step for Mg - 25 ppmw Fe in 0.1 M NaCl solution. Left: Mg dissolution rate ($i_{Mg}$); and right: HER rate ($i_{H_2}$). The applied current ($|i_e|$) is shown for reference. Note the scale difference for the two curves.

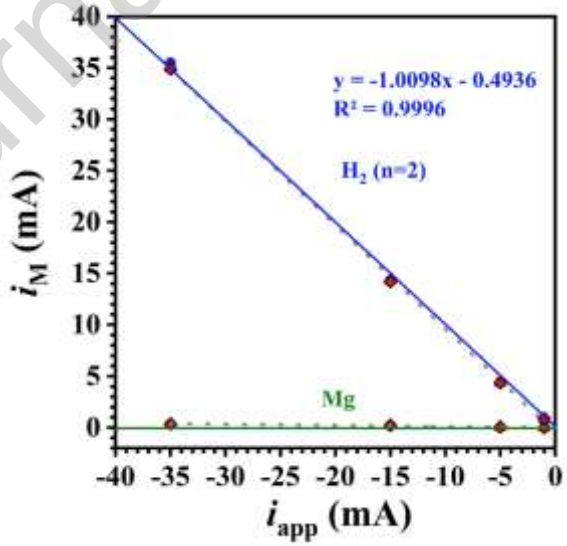


**Fig. 3.** Variation of $i_{H_2}$ and $i_{Mg}$ as a function of $i_{app}$ in the cathodic domain from **Fig. 2**. The dashed lines give a least squares fit to the data while the solid lines show the theoretical (n = 2) for HER and (n = 0) for Mg dissolution.

**Fig. 3** gives the relationship between $i_{H_2}$ vs. $i_{app}$ in the cathodic potential domain. The results confirm the accuracy of $i_{H_2}$ vs. $i_{app}$ for Mg, comparable to the results for the inert Pt electrode in Part I [21]. In fact, for the Mg electrode, the linearity was extended to below 5 mA which was not possible for Pt, perhaps due to the smaller surface area (0.5 $cm^2$) used in the previous work. The Mg dissolution rate, $i_{Mg}$, did vary with time as shown on the left hand side of **Fig. 2** (note scale difference), increasing with increasing absolute value of the applied cathodic current. While the origin of the cathodic Mg dissolution could not be established with certainty, it could simply represent the mechanical removal of previously formed oxides by the formation of hydrogen bubbles. The Mg dissolution rate in this potential domain remained negligible as compared to the HER rate and was not further investigated in this work.

*3.3. Anodic polarization and the negative difference effect*

The anodic galvanostatic experiments are shown in **Fig. 4** for the three alloys. Several points are immediately clear from inspection of these data. For all alloys, the Mg dissolution rate was relatively stable and followed closely the applied current as predicted by Faraday's law, assuming **Eq. 1**, n = 2. This is in agreement with the potentiodynamic results of **Fig. 1**. The HER rate was readily measurable for all applied currents and increased proportionally to the applied current, indicative of the NDE. The HER rate was noticeably less stable than for the cathodic experiments of **Fig. 2** at equivalent currents, especially for the higher Fe containing materials.

For the 25 ppmw Fe material, the HER rate was nearly constant on average although there was significantly more variation around the mean than was observed for an equivalent cathodic current (**Fig. 2**). The HER rate dropped down to near zero after the applied current was removed and the system returned to the open circuit potential for the 25 ppmw Fe material. For the higher Fe containing alloys, the HER rate increased with time during the galvanostatic pulse and did not return to the previous

open circuit value when the current was stopped but remained at a higher level. The most probable interpretation of this result is that the build-up of Fe in the corrosion products enhances the catalytic activity of the surface for hydrogen reduction. The effect is most apparent for the 220 ppmw Fe material as the initial HER rate was very low while the final rate was nearly equivalent to that of the 13000 ppmw Fe sample (2 ~ 7 mA).

The stoichiometric results for $i_{Mg}$ and $i_{H_2}$ vs. $i_{app}$, obtained from the anodic galvanostatic curves in **Fig. 4** are summarized in **Fig. 5**. Note that the red solid line indicates the hypothetical n = 2. The data presented in **Fig. 5** were obtained as a 200 s average early (800 to 1000 s) and late (1400 to 1600 s) in **Fig. 4**. The discrepancy between the two points therefore reflects the increase of the rate over a 600 s time period. The agreement between $i_{Mg}$ and $i_e$ in the anodic domain is clearly demonstrated with a $e^-/Mg^{2+}(aq)$ stoichiometry very close to 2 for the three alloys. For the Mg - 13000 ppmw, the lower currents should be related to excessive Mg dissolution, however, this was probably due to the significant open circuit corrosion rate observed for this material. There was little variation between the early and late measurements demonstrating the stability of the electrochemically driven Mg dissolution reaction, **Eq. 1**.

The HER rate also showed a consistent correlation with the applied current. For Mg - 25 ppmw Fe, a least squares fit to the data of demonstrates a correlation of $H_2/e^-$ of approximately 0.49. The absence of an apparent steady state for the 220 and 13000 ppmw Fe samples makes interpretation difficult. Nevertheless, the data sets give a nearly 1:1 relationship between $i_{H_2}$ and $i_{app}$ for the early time period, which increases as the background corrosion rate increases.

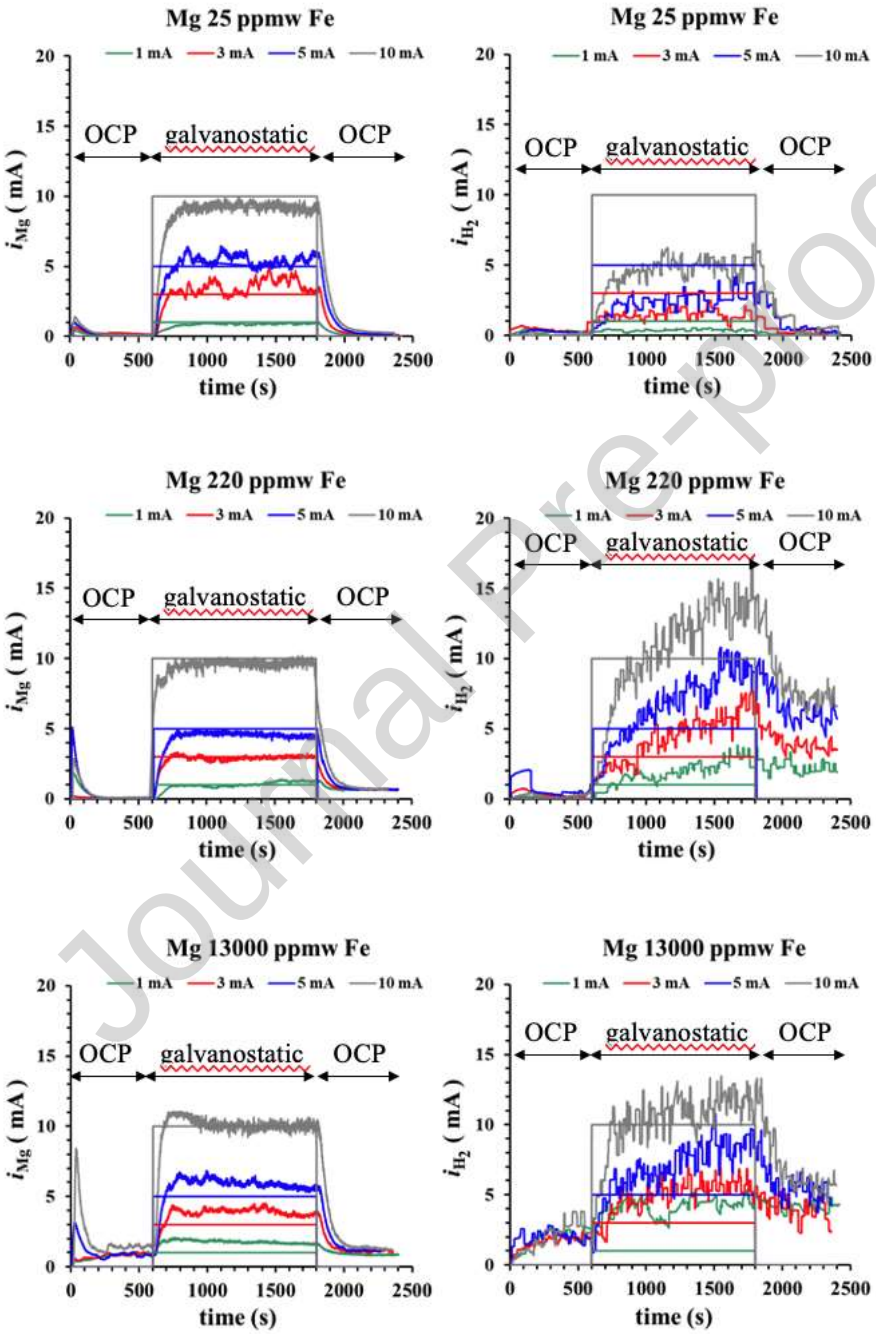


**Fig. 4.** Anodic galvanostatic dissolution Mg – Fe alloys at variable applied anodic current, $i_e$. Shown are the Mg dissolution rate ($i_{Mg}$, left) and HER rate ($i_{H_2}$, right). The rectangular curves show the applied current, $i_e$. The exposed surface area was 1 $cm^2$.

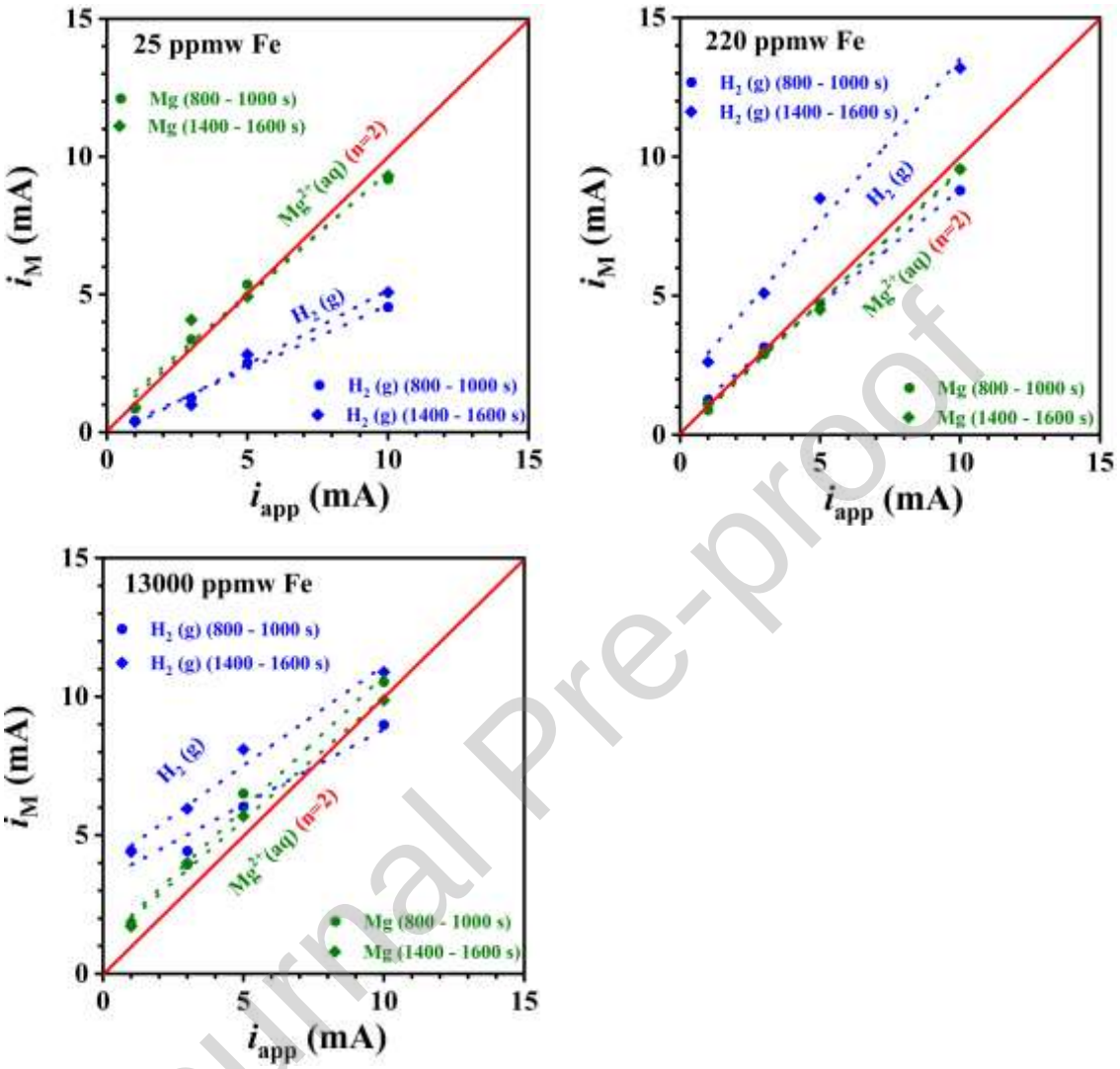


**Fig. 5.** HER and Mg dissolution rates expressed as equivalent currents ($i_{H_2}$ and $i_{Mg}$, respectively) as a function of the applied anodic current ($i_{app}$) from the galvanostatic experiments of **Fig. 4**. The red solid line is the hypothetical n = 2. The early (lower) and late (upper) rate of HER are shown as separate points. The exposed surface area was 1 $cm^2$.

### *3.4. Potentiostatic dissolution*

Potentiostatic experiments were performed (**Fig. 6**) with Mg - 25 ppmw Fe and Mg - 13000 ppmw Fe to represent the two extremes at anodic potentials of -1 V and 0 V vs. SCE. Throughout these experiments the anodic current was fairly stable indicating that the resistance changes were small, and as before, the Mg dissolution rate followed the

anodic current rather closely. The $i_e$, $i_{Mg}$, $i_{H_2}$ are presented as a function of potential on the potentiodynamic curves of **Fig. 1** demonstrating that the results are consistent with the potentiodynamic and the galvanostatic experiments. The 13000 ppmw Fe alloy showed a highly unstable HER rate while Mg dissolution rate was relatively stable. This result indicates that variations in the interfacial resistance and electrode surface area due to corrosion product films and growing hydrogen bubbles are actually quite small and do not play an important role in the kinetics of the reactions, at least on this time scale.

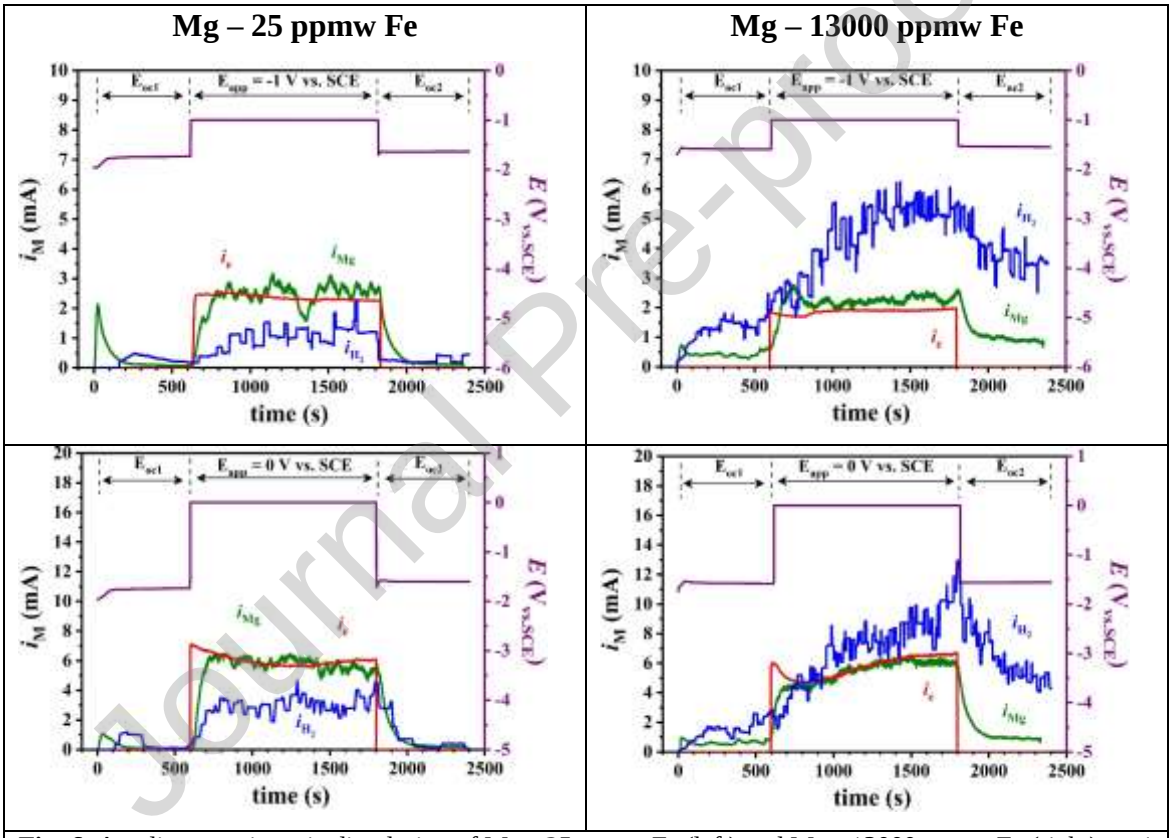


**Fig. 6.** Anodic potentiostatic dissolution of Mg - 25 ppmw Fe (left) and Mg - 13000 ppmw Fe (right) at -1 V vs. SCE (upper) and 0 V vs. SCE (lower). Shown are the Mg dissolution rate ($i_{Mg}$) and the HER rate ($i_{H_2}$) and the total current, ($i_e$). The exposed surface area was 1 $cm^2$.

*3.5. Spontaneous corrosion, repassivation, and the catalytic effect*

The steady increase in the HER rate at a constant applied anodic current and the resulting increase in the open circuit spontaneous corrosion rate was only observed for the higher Fe containing alloys. Notably, no enhancement in the Mg dissolution rate

was observed and even for the 13000 ppmw material, the Mg dissolution rate returned to its near zero initial value after the imposition of an anodic current (**Fig. 4**). These results are consistent with the hypothesis that the electrochemical dissolution of Mg (**Eq. 1**) proceeds by an independent mechanism than that of the HER (**Eqs. 5** and **6**) although they may be coupled indirectly. The electrochemical anodic current gives rise to predominantly dissolved $Mg^{2+}$ cations, while the HER would yield essentially solid oxidation products as in **Eqs. 5** and **6**.

The increasing HER rate profile as a function of the measurement time for the higher Fe content samples is probably due to the build-up of metallic Fe in the oxide film due to the selective oxidation of Mg, as Fe is well known for its catalytic properties for hydrogen evolution [16, 24, 25, 26]. The effect is most apparent for the 220 ppmw Fe because the surface concentration of Fe is initially low due to the low Mg dissolution rate in the first open circuit measurement. Therefore, the Fe build-up leads to a marked increase in active surface site for HER. For the 13000 ppmw Fe, the initial open circuit HER rate is already quite significant, probably due to the high initial Mg dissolution leading to form a metallic Fe enriched layer catalytic to HER. In this case, the effect of the Fe build-up throughout anodic polarization is less pronounced than the case of 220 ppmw Fe.

The decay of the HER and Mg dissolution rates following anodic polarization may be considered as a form of repassivation, as the activated surface returns to its original, less reactive state. The decrease of the Mg dissolution and HER rates represents a measure of the repassivation rate. This is shown in **Fig. 7** which compares the rates during open circuit potential (OCP) trace before (solid curves) and after (dashed curves) the LSV experiments of **Fig. 1**. For the latter, the t = 0 point is defined as the time at which the potential returns to open circuit. In all three cases the Mg dissolution rate profile is nearly identical and returns very close to its near zero initial value. The HER rate returns to its initial near zero value only for the 25 ppmw Fe alloy; the two others show a markedly enhanced HER rate. The solid red curve in **Fig. 7** is a trace of the Mg

dissolution rate for Mg - 25 ppmw Fe, offset to account for the enhanced background HER rate. From this analysis, it appears that the decay kinetics have not changed significantly, only the increase in the background HER rate.

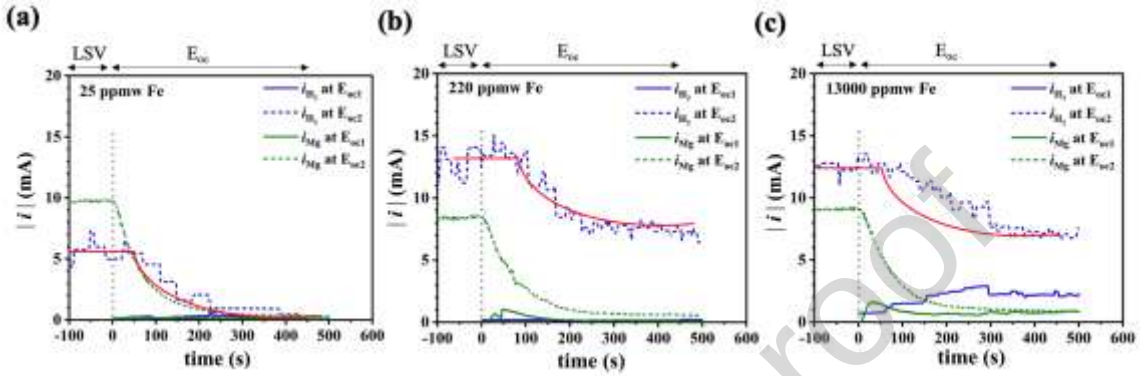


**Fig. 7.** Mg dissolution rate ($i_{Mg}$) and hydrogen evolution rate ($i_{H_2}$) before LSV ($E_{oc1}$, solid curves) and after LSV ($E_{oc2}$, dashed curves) (from **Fig. 1**) in a 0.1 M NaCl solution. The open circuit dissolution and HER rate profiles were recorded for 600 s for the three alloys as indicated. The solid red line curve gives the time variation of the HER for the 25 ppmw case, offset to account for the enhanced open circuit corrosion rate. For $E_{oc1}$, $t < 0$ indicates a time period when electrolyte was not in contact with the electrode; and for $E_{oc2}$ $t < 0$ indicates the last time period of the LSV measurement.

These results confirm that for materials containing noble impurities, the enhanced reactivity may be largely due to the build-up of those impurities during the anodic polarization. This would of course be the case for most practical Mg alloys in use. The enhancement of hydrogen evolution is more significant than Mg dissolution, however, indicating that the autocatalytic effect favors the formation of insoluble oxidation products over dissolved Mg ions.

The consistency of the Mg dissolution rate is shown in **Fig. 8** where the Mg dissolution rate has been normalized to the applied current, $i_{Mg} / i_{app}$. It is clear that within experimental error the profiles are nearly identical and the decay process is independent of the applied current. Also shown is the calculated decay rate that we would expect for the flow cell based on measurements and simulations of the residence time distribution of ions in the flow cell [27]. The result demonstrates that Mg leaching

from the flow cell is slower than would be the case based purely on hydrodynamics of the flow cell.

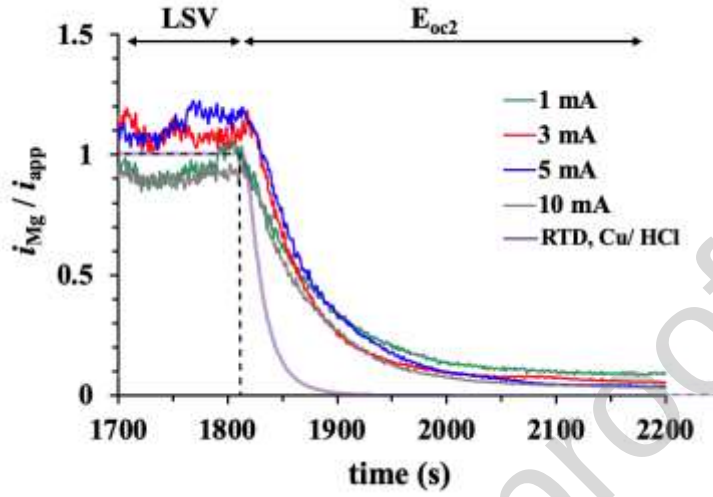


**Fig. 8.** Normalized Mg dissolution rate ($i_{Mg}$ / $i_{app}$) for Mg - 25 ppmw Fe in 0.1 M NaCl solution during the second OCP period following variable anodic galvanostatic exposures, from **Fig. 4**. The calculated decay predicted by previous evaluations of the flow cell residence time distributions (RTD) measured for nominally pure Cu in 1.0 M HCl with 1 mA galvanostatic pulse is shown in purple for comparison based on [27].

## 4. Discussion

A clear understanding of the stoichiometry of anodic Mg dissolution and $H_2$ generation is a necessary first step in clarifying the reaction mechanisms. **Table 2** compares the results of this study with that of experimental stoichiometric measurements prior to this work. Some caution is necessary in using this table in that the stoichiometery was in some case variable with time although the majority of the experiments were detemrined from average values after variable time periods. From inspection of the table, it is clear that the $e^-$ : $H_2$ mole ratio of 1 : 0.25 ($i_e$ : $i_{H_2}$ ≈ 1:0.5) for the purest sample (25-ppmw Fe, **Fig. 5**) is similar to the results obtained by the majority of researchers working with high purity Mg.

For the less pure materials (220 and 13000 ppmw Fe) the $e^-$ : $H_2$ mole ratio was ≈ 1 : 0.5 ($i_e$ : $i_{H_2}$ ≈ 1:1), but was not stable, increasing steadily during the experiment (see **Fig. 4**) reaching approximately 1:0.7 at longer times. The instability was especially

visible in the potentiostatic profiles although the 1:0.5 stoichiometry of $e^-$ : $Mg^{2+}$ was quite stable. This variation is reflected in the literature with values reaching $e^-$ : $H_2$ mole ratio ≈ 1 : 0.8 which also correlates with the Fe content of the materials and the applied anodic current. The high variability indicates that the HER was not directly related to the electrochemical current, the counter example, being cathodic hydrogen reduction the expected $e^-$ : $H_2$ mole ratio of 1 : 0.5 was obtained under all conditions of this work.

The important contribution of this work is to confirm the previously reported $e^-$ : $Mg^{2+}$(aq) mole ratio = 1 : 0.5 over a wide range of Mg purity and applied current/potential conditions. This stoichiometry was observed with good reproducibility over all the conditions of these experiments and was stable throughout the experiments, and independent of the HER. There is little data in the literature with which to compare this result other than from previous publications of the present authors, since the measurement requires an online analysis of the dissolved Mg. Also many authors use $Mg(OH)_2$ saturated electrolytes for these experiments in which case $Mg^{2+}$ dissolution is unlikely and would be unmeasureable in any case. A similar stoichiometry was observed in Rossrucker *et al*. [15] using ICP mass spectrometer although the point was not discussed therein.

This n = 2 stoichiometry suggests that the formation of aqueous $Mg^{2+}$ ions occurs *via* an n = 2 mechanism (**Eq. 1**) with a near 100% faradaic efficiency in unbuffered 0.1 M NaCl. It follows from a mass-charge balance that of Eq. 4, that if $|i_e| = i_{Mg^{2+}}$, then $i_{H_2} = i_{Mg(II)\text{-}ox}$. Therefore, if Mg dissolution occurred *via* a direct electrochemical reaction, it would follow that the hydrogen evolution reaction must occur by a different mechanism involving the direct reaction of Mg with $H_2O$ (**Eq. 5** and/or **6**) leading to the formation of insoluble Mg corrosion products [13, 14].

Indeed, the reduction of $H_2O$ in the unbuffered solution would lead to an increase in interfacial pH favoring the precipitation of Mg hydroxides and oxides, and would not be detected by ICP-AES. Fe impurities were shown to have a strong accelerating effect on

the HER but did not affect the stoichiometry of the electrochemical dissolution mechanism, $e^-/Mg^{2+}(aq)$.

By contrast, electrochemically driven Mg dissolution (**Eq. 1**), with the cathodic reaction localized on the counter electrode, would not produce a similar pH increase and therefore, we would expect the dominant product to be $Mg^{2+}(aq)$ ions (**Eq. 1**) that may be detected in solution by ICP-AES. It is probable that this reaction occurs across the naturally formed oxide / hydroxide film. The breakdown of this naturally protective film would result in defects where metallic Mg(0) comes into contact with the electrolyte, a direct reaction will occur, **Eq. 5** and/or **6**. This would give rise to the hydrogen evolution reaction which would increase with increasing potential (*i.e.*, the NDE). This reaction would not be detected directly by ICP-AES nor contribute to the electrochemical current. This demonstrates the need for simultaneous gravimetric $H_2$ and dissolved Mg measurement to quantify the contribution of $H_2$ evolution rate for a complete mass-charge balance of Mg corrosion.

The objective of this article is to demonstrate the methodology of real time kinetics for hydrogen evolution and Mg dissolution by determining the stoichiometry as a function of time for anodic Mg dissolution. Nevertheless, this stoichiometry of the reaction process sets a boundary condition for any mechanistic speculation. As was discussed in Lebouil *et al.* [13,14] these observations are in good agreement with a very early explanation of the NDE proposed by U.R. Evans in 1946 [28], and elaborated by Robinson and King [29] and Tunold *et al.* [30] in 1977. It is well known that when Mg is exposed to water, a passive film of hydroxide and/or oxide forms spontaneously. This film serves to separate the metallic Mg from the aqueous solution as indicated by the typical corrosion potential in acidic solution is generally much more positive than the thermodynamic -2.38 V vs. SHE [31]. In this hypothesis, the NDE arises when, under anodic polarization, the passive film breaks down locally and the Mg reacts directly with water. This produces $Mg^{2+}$, $H_2$ and $OH^-$, with the resulting pH increase leading to the precipitation of $Mg(OH)_2$.

The latter would most likely correspond to the black film associated with the cathodic areas observed on the surface [32, 33]. In other words, the NDE would be explained by what is analogous to a pitting mechanism. In fact, hydrogen production from pits has been observed on Al [34], Fe-20Cr, and stainless steel even for imposed potentials as noble as 1.4 V vs. SHE [35]. This mechanism has been elaborated in detail for the NDE on Al [5]. In this hypothesis, we would therefore expect to see an NDE effect on any metal for which the pitting potential (or the potential at the bottom of a pit) is below the thermodynamic potential of hydrogen formation. As a consequence, the only thing that makes Mg unique is the degree to which hydrogen production is observed which is no doubt a result of the aforementioned thermodynamic affinity to react with water, coupled with the poorly passivating nature of most Mg corrosion products. This effect is enhanced by the presence of noble impurities (Fe in this work) which have been shown to have an accelerating effect on anodic hydrogen production (NDE) [16] and the accelerating effect continues even after the polarization.

**Table 2.** Summary of previous stoichiometric measurements for the anodic dissolution of Mg under similar conditions to this work.

* = Authors stated in the paper; ** = authors gave a figure indicating the stoichiometry; *** = authors gave a figure, stoichiometry calculated by us; and $^{T}$: Variable with time

| Mg purity | Electrolyte | Anotic current / mA cm$^{-2}$ | $e^-$ : $H_2$ | $e^-$ : $Mg^{2+}$ (aq) | $H_2$ : $Mg^{2+}$(aq) | $e^-$ : Mg | $H_2$ : Mg | Ref. |
|---|---|---|---|---|---|---|---|---|
| | | | | Dissolved Mg (AESEC) | | Mg total oxidation (mass loss) | | |
| Stoichiometry based on charge ($e^-$), dissolved Mg (Mg(aq)) and $H_2$; or charge and dissolved Mg | | | | | | | | |
| *25 ppmw Fe* | *0.1 M NaCl* | *1 ~ 10* | *≈1:0.25* | *≈1:0.5* | *≈1:2* | - | - | *This work* |
| *220 ppmw Fe* | | | *≈1:0.5$^{T}$* | | *≈1:1* | - | - | |
| *13000 ppmw Fe* | | | *≈1:0.5$^{T}$* | | *≈1:1* | - | - | |
| 280 ppm Fe | 0.01 M NaCl | ~ 10 | ***1:0.7 | ***1:0.6 | ***1:0.86 | - | - | [13] |
| 280 ppm Fe | 0.01 M NaCl | ~ 1 | ***1:0.5 | ***1:0.5 | ***1:1 | - | - | [14] |
| 45 ppm Fe | 0.03 M NaCl | 0.2 ~ 0.8 | - | *1:0.5 | - | - | - | [12] |
| 17 ppm Fe | 0.01 M | 0.2 ~ 2.3 | - | *1:0.5 | - | - | - | [15] |
| Stoichiometry based on $H_2$ and charge | | | | | | | | |
| < 10 ppm Fe | 0.1 M NaCl | 1 ~ 50<br>75 | **1:0.25<br>*≈1:0.1 | - | - | - | - | [36] |
| 0.1, 40 ppm Fe | 0.1 M NaCl | 1 ~ 75 | *1:0.2 ~ 0.3 | - | - | - | - | [24] |
| 0.1 ppm Fe | 0.1 ~ 2 M NaCl | 1 ~ 4 | *1:0.22 | - | - | - | - | [37] |
| 40 ppm Fe | 0.1 M citric buffer (pH = 3) | 0 ~ 75 | *1:0.28 | - | - | - | - | [38] |
| 99.98 % Mg | 0.1 M NaCl | 1 ~ 25 | *1:0.33 | - | - | - | - | [20] |
| Stoichiometry based on $H_2$, charge, and mass loss of Mg; or charge and mass loss of Mg | | | | | | | | |
| 0.0015 wt.% Fe | 1 M NaCl | 0.5 ~ 16 | - | - | - | - | *1:1.96 | [39] |
| 20 ppm Fe | 3.5 wt.% NaCl with sat. $Mg(OH)_2$ | 0.1 ~ 100 | - | - | - | *1:0.69 | ***1:2.9 | [40] |
| 0.003 wt.% Fe | 3.5 wt.% NaCl | 0.01 ~ 100 | *1:0.67 | - | - | - | ***1:2.5 | [41] |
| 0.024 wt.% Fe | 0.01 M NaCl | - | ***1:0.78 | - | - | - | ***1:2.2 | [42] |
| 80 ppmw Fe | 0.6 M NaCl with/without sat. $Mg(OH)_2$ | Potentio-static | **1:0.43 | - | - | 1:1 | **≈1:2.2 | [43] |

## 5. Conclusions

In this study, the stoichiometry of anodic Mg dissolution and hydrogen evolution were investigated using a novel approach incorporating element-resolved electrochemistry (AESEC) coupled with a gravimetric hydrogen detection system. The stoichiometry was investigated over a wide range of applied anodic currents and potentials, for Mg specimens with widely varying Fe impurity concentrations.

- It was determined that Mg dissolution closely follows the anodic faradaic current, with n = 2, consistent with $Mg \rightarrow Mg^{2+}(aq) + 2\ e^-$, for all currents and potentials, whilst being independent of the Fe impurity concentration.
- The negative difference effect (NDE) increased with increasing anodic current. Hydrogen evolution was markedly enhanced for Mg when the Fe impurity concentrations were appreciable. However, even the most pure material tested (25 ppmw Fe) revealed a significant HER rate during anodic polarization. The HER rate in this case is stable and returns to nearly the original open circuit value once the applied current is removed.
- By contrast, the Fe enriched specimens showed a steadily increasing HER rate which remained elevated, even following the removal of an applied anodic polarization. However, Mg dissolution was not enhanced or affected by the presence of Fe, demonstrating that the NDE results almost exclusively in the formation of insoluble Mg oxidation products, in contrast to the applied anodic current which results almost exclusively in dissolved $Mg^{2+}$ ions.
- These results are consistent with a mechanism involving an electrochemical Mg dissolution mechanism across an intact protective film, with hydrogen evolution occurring at areas where the film has broken down and $H_2O$ reacts directly with Mg to form insoluble corrosion products.



## Acknowledgements

Author Baojie Dou would like to express his gratitude to China Scholarship Council (CSC) for financial support.

**Declaration of interests**

☒ The authors declare that they have no known competing financial interests or personal relationships that could have appeared to influence the work reported in this paper.

☐The authors declare the following financial interests/personal relationships which may be considered as potential competing interests:

# Highlights

- The rates of hydrogen evolution, Mg dissolution, and electron transfer were measured simultaneously in real time during the anodic polarization of magnesium.
- The $Mg^{2+}/e^-$ ratio is equal to an expected 1:2 consistent with a two-electron transfer mechanism for dissolution.
- The $Mg^{2+}/H_2$ was 2:1 for the nominally pure (25 ppmw Fe) Mg material; but was approximately 1:1 and unstable for higher Fe content.
- For the high Fe containing specimens, the corrosion rate was enhanced following anodic polarization. This effect was not observed for nominally pure Mg.
- The kinetics of spontaneous repassivation of Mg following anodic polarization were obtained.



**REFERENCE**

[1] W. Beetz, "On the development of hydrogen from the anode", *Phil. Mag.*, **32** (1866) 269-278. https://doi.org/10.1080/14786446608644179

[2] S. Thomas, N.V. Medhekar, G.S. Frankel, and N. Birbilis, "Corrosion mechanism and hydrogen evolution on Mg*", Curr. Opin. Solid State Mater. Sci.*, **19** (2015) 85–94. https://doi.org/10.1016/j.cossms.2014.09.005

[3] J.A. Yuwono, N. Birbilis, C.D. Taylor, K.S. Williams, A.J. Samin, and N.V. Medhekar, "Aqueous electrochemistry of the magnesium surface: Thermodynamic and kinetic profiles" *Corros. Sci.*, **147** (2019) 53-68. https://doi.org/10.1016/j.corsci.2018.10.014

[4] M. Esmaily, J.E. Svensson, S. Fajardo, N. Birbilis, G.S. Frankel, S. Virtanen, R. Arrabal, S. Thomas, and L.G. Johansson, "Fundamentals and advances in magnesium alloy corrosion", *Prog. Mater. Sci.*, **89** (2017) 92–193. https://doi.org/10.1016/j.pmatsci.2017.04.011

[5] Y. Yu, and Y. Li "New insight into the negative difference effect in aluminium corrosion using in-situ electrochemical ICP-OES", *Corros. Sci.*, **168** (2020) 108568. https://doi.org/10.1016/j.corsci.2020.108568

[6] R.L. Liu, S. Thomas, J.R. Scully, G. Williams, and N. Birbilis, "An experimental survey of the cathodic activation of metals including Mg, Sc, Gd, La, Al, Sn, Pb, and Ge in dilute chloride solutions of varying pH", *Corrosion*, **73**(5) (2017) 494-505. https://doi.org/10.5006/2282

[7] T. Zhang, Z. Tao, and J. Chen "Magnesium-air batteries: from principals to applications", *Mater. Horiz.*, **1** (2014) 196-206. https://doi.org/10.1039/C3MH00059A

[8] H.D. Yoo, I. Shterenberg, Y. Gofer, G. Gershinsky, N. Pour, and D. Aurbach, "Mg rechargeable batteries: an on-going challenge", *Energy Environ. Sci.*, **6** (2013) 2265–2279. https://doi.org/10.1039/C3EE40871J

[9] B. Peng, and J. Chen, "Functional materials with high-efficiency energy storage and conversion for batteries and fuel cells", *Coord. Chem. Rev.*, **253** (2009) 2805–2813. https://doi.org/10.1016/j.ccr.2009.04.008

[10] J. Chen, and F. Cheng, "Combination of lightweight elements and nanostructured materials for batteries", *Acc. Chem. Res.*, **42** (2009) 713–723. https://doi.org/10.1021/ar800229g

[11] G. Song, A. Atrens, D. St John, J. Nairn, and Y. Lit, "The Electrochemical Corrosion of Pure magnesium in 1 N NaCl", *Corros. Sci.*, **39**(5) (1997) 855-875. https://doi.org/10.1016/S0010-938X(96)00172-2

[12] J. Światowska, P. Volovitch, and K. Ogle, "The anodic dissolution of Mg in NaCl and $Na_2SO_4$ electrolytes by atomic emission spectroelectrochemistry", *Corros. Sci.*, **52** (2010) 2372-2378. https://doi.org/10.1016/j.corsci.2010.02.038

[13] S. Lebouil, O. Gharbi, P. Volovitch, and K. Ogle, "Mg dissolution in phosphate and chloride electrolytes: Insight into the mechanism of the negative difference effect", *Corrosion*, **71**(2) (2015) 234-241. https://doi.org/10.5006/1459

[14] S. Lebouil, A. Duboin, F. Monti, P. Tabeling, P. Volovitch, and K. Ogle, "A novel approach to on-line measurement of gas evolution kinetics: Application to the negative difference effect of Mg in chloride solution", *Electrochim. Acta,* **124** (2014) 176-182 (2014). https://doi.org/10.1016/j.electacta.2013.07.131

[15] L. Rossrucker, K. J. J. Mayrhofer, G. S. Frankel, and N. Birbilis, "Investigating the real time dissolution of Mg using online analysis by ICP-MS", *J. Electrochem. Soc.,* **161** (2014) C115-C119. https://doi.org/10.1149/2.064403jes

[16] S. Thomas, O. Gharbi, S.H. Salleh, P. Volovitch, K. Ogle, and N. Birbilis, "On the effect of Fe concentration on Mg dissolution and activation studied using atomic emission spectroelectrochemistry and scanning electrochemical microscopy", *Electrochim. Acta,* **210** (2016) 271-284. https://doi.org/10.1016/j.electacta.2016.05.164

[17] S. Fajardo, O. Gharbi, N. Birbilis, and G. S. Frankel, "Investigating the effect of ferrous ions on the anomalous hydrogen evolution on magnesium in acidic ferrous chloride solution", *J. Electrochem. Soc.,* **165**(13) (2018) C916-C925. https://doi.org/10.1149/2.0951813jes

[18] M. Curioni, "The behaviour of magnesium during free corrosion and potentiodynamic polarization investigated by real-time hydrogen measurement and optical imaging", *Electrochim. Acta,* **120** (2014) 284-292. https://doi.org/10.1016/j.electacta.2013.12.109

[19] M. Curioni, F. Scenini, T. Monetta, and F. Bellucci, "Correlation between electrochemical impedance measurements and corrosion rate of magnesium investigated by real-time hydrogen measurement and optical imaging", *Electrochim. Acta,* **166**(1) (2015) 372-384. https://doi.org/10.1016/j.electacta.2015.03.050

[20] S. Fajardo, and G.S. Frankel, "Gravimetric method for hydrogen evolution measurements on dissolving magnesium", *J. Electrochem. Soc.,* **162** (2015) C693-C701. https://doi.org/10.1149/2.0241514jes

[21] B. Dou, X. Li, J. Han, K. Ogle, "*Operando* kinetics of hydrogen evolution and elemental dissolution I: The dissolution of galvanized steel in hydrochloric acid", *Corros. Sci.,* **214** (2023) 111007. https://doi.org/10.1016/j.corsci.2023.111007

[22] J. Han, and K. Ogle, "Communication—Hydrogen evolution and elemental dissolution by combined gravimetric method and atomic emission spectroelectrochemistry", *J. Electrochem. Soc.,* **166**(11) (2019) C3068-C3070. https://doi.org/10.1149/2.0091911jes

[23] K. Ogle, "Atomic emission spectroelectrochemistry real-time rate measurements of dissolution, corrosion, and passivation", *Corrosion,* **75**(12) (2019) 1398-1419. https://doi.org/10.5006/3336

[24] S. Fajardo, and G.S. Frankel, "Effect of impurities on the enhanced catalytic activity for hydrogen evolution in high impurity magnesium", *Electrochim. Acta,* **165** (2015) 225-267. https://doi.org/10.1016/j.electacta.2015.03.021

[25] N. Birbilis, A.D. King, S. Thomas, G.S. Frankel, and J.R. Scully, "Evidence for enhanced catalytic activity of magnesium arising from anodic dissolution", *Electrochim. Acta,* **132** (2014) 277-283 (2014). https://doi.org/10.1016/j.electacta.2014.03.133

[26] S. Fajardo, O. Gharbi, N. Birbilis, and G. S. Frankel, "Investigating the effect of ferrous ions on the anomalous hydrogen evolution on magnesium in acidic ferrous chloride solution", *J. Electrochem. Soc.*, **165**(13) (2018) C916-C925. https://doi.org/10.1149/2.0951813jes

[27] V. Shkirskiy, P. Maciel, J. Deconinck, and K Ogle, "On the time resolution of the atomic emission spectroelectrochemistry method", *J. Electrochem. Soc.*, **163**(3) (2016) C37-C44. https://doi.org/10.1149/2.0991602jes

[28] U.R. Evans, Metallic Corrosion, Passivity, and Protection, 2nd Edition, (London, UK: Edward Arnold & Co., 1946) 814.

[29] J.F. Robinson, and P.F. King, "Electrochemical behavior of the magnesium anode", *J. Electrochem. Soc.*, **108** (1961) 36. https://doi.org/10.1149/1.2428007

[30] R. Tunold, H. Holtan, M.B. Hagg Berge, A. Lasson, and R. Steen-Hansen, "The corrosion of magnesium in aqueous solution containing chloride ions", *Corros. Sci.*, **17** (1977) 353-365. https://doi.org/10.1016/0010-938X(77)90059-2

[31] A. Atrens, G.-L. Song, F. Cao, Z. Shi, and P.K. Bowen, "Advances in Mg corrosion and research suggestions", *J. Magnes. Alloy.*, **1** (2013) 177-200. https://doi.org/10.1016/j.jma.2013.09.003

[32] G. Williams, N. Birbilis, and H.N. McMurray, "The source of hydrogen evolved from a magnesium anode", *Electrochem. Commu.*, **36** (2013) 1-5. https://doi.org/10.1016/j.elecom.2013.08.023

[33] G. Williams, and H.N. McMurray, "Localized corrosion of magnesium in chloride-containing electrolyte studied by a scanning vibrating electrode technique", *J. Electrochem. Soc.*, **155** (2008) C340-C349. https://doi.org/10.1149/1.2918900

[34] G. S. Frankel, "The growth of 2-D pits in thin film aluminum" *Corros. Sci.*, **30** (1990) 1203. https://doi.org/10.1016/0010-938X(90)90199-F

[35] H. W. Pickering, and R. P. Frankenthal, "On the mechanism of localized corrosion of iron and stainless steel", *J. Electrochem. Soc.*, **119** (1972) 1297. https://doi.org/10.1149/1.2403982

[36] G.S. Frankel, A. Samaniego, and N. Birbilis, "Evolution of hydrogen at dissolving magnesium surfaces", *Corros. Sci.*, **70** (2013) 104-111. https://doi.org/10.1016/j.corsci.2013.01.017

[37] S. Fajardo, C.F. Glover, G. Williams, and G.S. Frankel, "The source of anodic hydrogen evolution on ultra high purity magnesium", *Electrochim. Acta*, **212** (2016) 510-521. https://doi.org/10.1016/j.electacta.2016.07.018

[38] S. Fajardo, C.F. Glover, G. Williams, and G.S. Frankel, "The evolution of anodic hydrogen on high purity magnesium in acidic buffer solution", *Corrosion*, **73**(5), 2017, 482-493. https://doi.org/10.5006/2247

[39] T.R. Tomaz, C.R. Weber, T. Pelegrini Jr., L.F.P. Dick, and G. Knörnschild, "The negative difference effect of magnesium and the AZ91 alloy in chloride and stannate-containing solutions", *Corros. Sci.*, **52** (2010) 2235-2243. https://doi.org/10.1016/j.corsci.2010.03.010

[40] Z. Shi, J.-X. Jia, and A. Atrens, "Galvanostatic anodic polarization curves and galvanic corrosion of high purity Mg in 3.5% NaCl saturated with $Mg(OH)_2$", *Corros. Sci.*, **60** (2012) 296-308. https://doi.org/j.corsci.2011.12.002

[41] Y. Li, Z. Shi, X. Chen, and A. Atrens, "Anodic hydrogen evolution on Mg", *J. Mg & Alloys*, **9** (2021) 2049-2062. https://doi.org/10.1016/j.jma.2021.09.002

[42] S. Bender, J. Goellner, and A. Atrens, "Corrosion of AZ91 in 1N NaCl and the mechanism of magnesium corrosion", *Adv. Engin. Mater.*, 1**0(**6), (2008) 583-587. https://doi.org/10.1002/adem.200800005

[43] T.W. Cain, I. Gonzalez-Afanador, N. Birbilis, and J.R. Scully, "The role of surface films and dissolution products on the negative difference effect for magnesium: comparison of $Cl^-$ versus $Cl^-$ free solutions", *J. Electrochem. Soc.*, **164**(6), 2017) C300-C311. http://doi.org/10.1149/2.1371706jes

Graphical abstract

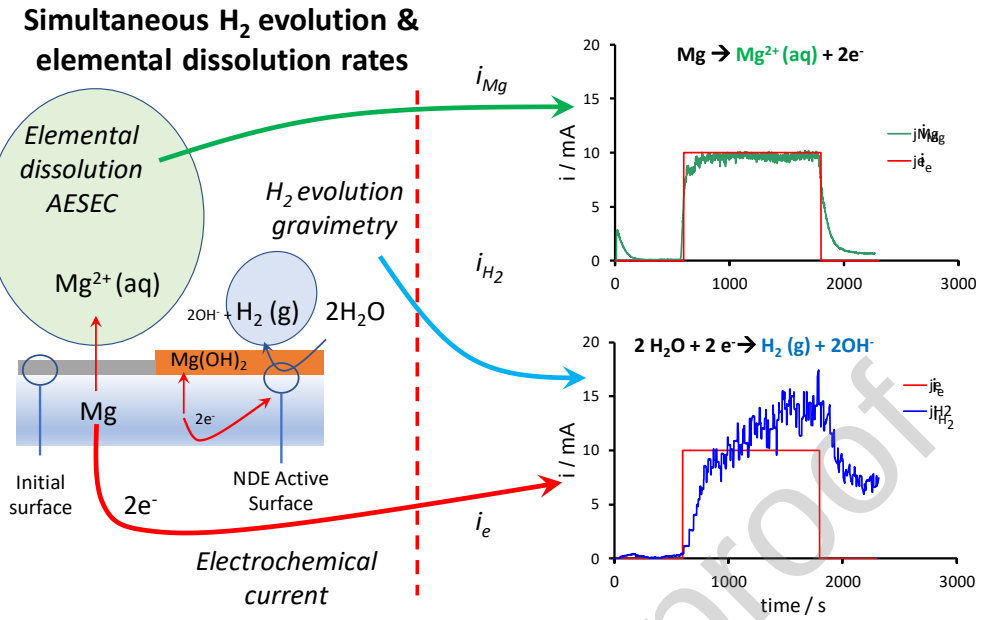


**CRediT authorship contribution statement**

BD: Investigation, methodology, visualization, writing – first draft, validation.

XL: Methodology, investigation

JH: Methodology, investigation, visualization, validation, writing, review & editing

ND: Review & editing, validation, resources

KO: Methodology, visualization, writing, review & editing, validation, supervision, resources, funding acquisition.

1